REX: An Analytical Tool for Reactor Operating Envelope Expansion Through Fuel-Clad Thermo-Mechanics

Nicholas J Fassino, Anna Erickson*

Georgia Institute of Technology, Woodruff School of Mechanical Engineering, Nuclear and Radiological Engineering Program, 770 State Street, Atlanta, GA 30332, USA

ARTICLE INFO

Keywords:
operating envelope
reactor design
fuel-cladding thermo-mechanics
mechanical failure
Serpent

ABSTRACT

REX, an analytical reactor design tool for the identification and expansion of reactor operating envelopes, is introduced and detailed. Written in MATLAB, REX takes core geometries and axially discretized detector and depletion output from the Serpent neutron transport code and performs full-core, pin-specific thermal-hydraulic and thermo-mechanical calculations. REX identifies the operating envelopes of advanced, solid-fuel nuclear reactors on the basis of their fuel-cladding, fuel-gas, and coolant-cladding interfacial thermo-mechanics. It iteratively pushes coolant inlet temperatures and modifies fuel pin geometries to induce mechanical failure in their original cladding materials at the fullest extent of their fuel cycle lengths and permissible coolant inlet temperatures. It then attempts to expand their operating envelopes by determining the mechanical responses of alternative cladding materials under the same geometric conditions. The result of the REX calculation sequence is a set of 5-D variables describing the temperatures, pressures, geometries, and mechanics of the core as functions of assembly, fuel pin, axial zone, depletion step, and coolant inlet temperature for each candidate cladding material with the limiting fuel pin geometry for the original material.

1. Introduction

A major impediment to the operation of several solid-fuel reactor concepts is the performance of their fuel cladding materials [1]. In light-water reactors, accident conditions can result in prohibitive cladding oxidation. In several advanced reactor systems, high-temperature corrosive coolants, for example lead and lead-bismuth, can lead to damage of traditional cladding materials—relying on a protective oxide layer—unless coolant velocity and temperatures are limited [2, 3, 4]. The implementation of alternative cladding materials could mitigate these issues, relax coolant velocity constraints, and permit the coolant to deliver additional heat to the power conversion system, thereby expanding the operating envelopes of these reactor designs.

In this work, the operating envelope of a nuclear reactor is described as the set of neutronic, thermal-hydraulic, and thermo-mechanical conditions tolerable by reactor materials in the active region of the core. While a plethora of computational tools and subcodes such as FALCON [5] and MATPRO [6] have been developed to accurately analyze the performance of nuclear fuels and their effects on the reactor operating envelope, none perform the function of comparing sets of results and identifying potential means of operating envelope expansion through fuel pin geometry manipulation. For example, the Fuel Rod Integral Performance Analysis Code (FRIPAC), developed by China Nuclear Power Technology Research Institute Co. Ltd, utilizes a suite of models to predict PWR fuel pin behaviors during steady-state and power-ramp conditions [7]. FRAPCON, a computer code for the calculation of steady-state thermal-mechanical behavior of oxide fuel rods for high burnup, developed by Pacific Northwest National Laboratory [8], is designed to perform steady-state fuel rod calculations and generate inputs for its associated transient analyses code FRAPTRAN. BISON, a finite element-based nuclear fuel performance code developed with the MOOSE framework by Idaho National Laboratory, can efficiently solve problems pertaining to LWR fuel rods, TRISO fuels, metallic fuels, and plate fuels [9]. ALCYONE, a multidimensional fuel performance code, solves coupled equations describing PWR fuel rod thermo-mechanics and chemical-physics and is capable of 1.5-D, 2-D, and 3-D modeling schemes for full fuel rod, fuel pellet fragment, and mid-pellet plane problems, respectively [10]. While all of these advanced codes accurately describe fuel pin behavior, they do not natively and dynamically iterate on fuel pin geometries for thermo-mechanical operating envelope identification and expansion. Additionally, these codes were designed for LWR analysis and have not been validated for reactor designs with exotic coolants.

This study introduces and describes REX, an analytical reactor design tool developed to fill this need by comparing the operating envelopes of advanced reactor designs outfitted with a variety of candidate cladding materials. Written in MATLAB, REX performs a sequence of core-wide, pin-specific thermal-hydraulic and thermo-mechanical calculations to determine the mechanical stresses experienced by a candidate cladding material, manipulate fuel pin geometries to the point where these stresses prohibit reactor operation, then test the performance of alternative cladding materials under originally prohibitive conditions. Similar to the codes mentioned previously, REX considers discrete axial fuel subdivisions, which are then further discretized into radially concentric rings [7]. This 1.5-dimensional discretization is used to calculate coolant, cladding, and fuel temperature profiles, fuel and cladding deformations, and pressures at

*Corresponding author, 0000-0002-3276-4414
ORCID(s):

the coolant-clad, fuel-clad, and gas-clad interfaces. Once this calculation is completed for every fuel pin in the core, REX moves on to the next depletion step and repeats the calculation. At the end of the fuel cycle, REX will increase the coolant inlet temperature by a specified quantity, and repeat the entire fuel cycle calculation sequence to retrieve a pushed operating envelope. Once it reaches a maximum allowable coolant inlet temperature, REX seeks out mechanical failure of the original cladding by modifying fuel pin geometries to the point where cladding effective stresses exceed the maximum allowable stress, which is selected as the yield strength for ductile materials, and fracture stress for brittle materials. The original cladding is then replaced with an alternative cladding material, and the thermal-hydraulic and thermo-mechanical calculations are repeated with the new fuel pin geometries. Survival of an alternative cladding material under the same set of conditions that resulted in failure of the original material suggests operating envelope expansion, assuming reactor safety conditions are satisfied.

2. REX Methodology

2.1. Overview

REX uses several input parameters to perform a series of pin-specific thermal-hydraulic and thermo-mechanical calculations. The inputs for REX are detailed in Table 1. Among these inputs are pin-specific fission rates calculated with Serpent 2, a three-dimensional, continuous energy, Monte Carlo neutron transport code [11]. This Serpent simulation is executed separately from REX and must score fission rates in each assembly with the lattice detector option. REX normalizes these fission rates with the core nominal power to produce effective pin fission powers indexed to each assembly, fuel pin, and axial zone. An additional index, the depletion step, is produced if the built-in depletion capability of Serpent 2 is used. After all thermal-hydraulic and thermo-mechanical calculations are completed for the final depletion step, the coolant inlet temperature is increased by 50 K and the entire sequence is repeated from the initial depletion step. This iterative sequence is repeated until the maximum coolant outlet temperature is expected to exceed either the coolant boiling point or the cladding temperature limit at the next iteration. The result of this iterative sequence is a set of 5-D operating envelope parameters indexed to assembly, fuel pin, axial zone, depletion step, and coolant inlet temperature. The complete list of parameters calculated by REX is provided in Table 2.

After collecting these 5-D variables, REX performs a series of checks detailed in Sec. 2.4 and dynamically modifies the fuel-clad gap width and cladding thickness. The cold fuel radius is never modified in order to preserve the neutronics from the initial Serpent simulation. REX then determines the operating envelope of the reactor with the modified fuel pin geometries, then repeats the checks and adjustments. This iterative sequence is cycled until the effective stress on the original cladding material exceeds its maximum allowable stress at only the final depletion and coolant inlet temperature steps, ensuring the operational limit of the original cladding is reached. REX then replaces the original cladding with specified alternative materials and evaluates the reactor thermo-mechanics with the new cladding materials and fuel pin geometries.

The REX approach is summarized in Fig. 1.

2.2. Thermal Hydraulics

2.2.1. Subchannel Temperatures

REX divides each subchannel in the reactor core into discrete axial segments, with the number of axial zones defined by the detector inputs in the corresponding Serpent model. In each axial volume, REX calculates the temperatures listed in Table 2 by assuming 1-D heat conduction across the fuel element. The fuel pin and its labeled regions are illustrated in Fig. 2. The temperature of the bulk coolant, cladding outer surface, cladding inner surface, fuel surface, and fuel centerline are labeled as T_∞, T_{co}, T_{ci}, T_f, and T_{cl}, respectively.

REX makes the following assumptions in calculating subchannel temperatures:

(1) No heat conduction occurs in the axial direction. This is due to the fact that the temperature gradient in a fuel pin is much higher in the radial direction than in the axial direction [12].
(2) Power density within an axial zone is uniform across the fuel radius.
(3) No crossflow: coolant only flows axially upward in an assembly.

REX calculates T_∞, T_{co}, and T_{ci} with Eqns. 1–3 and the aforementioned assumptions for each axial segment:

$$T_\infty = T_{cool,in} + \frac{q'''V}{2\dot{m}_{sub}c_p} \tag{1}$$

$$T_{co} = \frac{1}{2}\frac{r_f^2 q'''}{r_{co}h} + T_\infty \tag{2}$$

$$T_{ci} = \frac{r_f^2 q'''}{2}\frac{log\left(\frac{r_{co}}{r_{ci}}\right)}{k_{clad}} + T_{co} \tag{3}$$

where q''' is the power density, V is the fuel volume, $\dot{m}_{sub}$ is the mass flow rate of the coolant in the subchannel, c_p is the coolant isobaric specific heat, $T_{cool,in}$ is the coolant inlet temperature, r_f is the fuel radius, h is the convective heat transfer coefficient of the coolant, r_{co} and r_{ci} are the cladding outer and inner radii, respectively, and k_{clad} is the thermal conductivity of the cladding.

If a fuel-clad gap exists, REX assumes it is occupied by a mixture of a fill gas and fission product gases that appear with burnup. The identity of the fill gas is specified as input and the atom densities of fission product gases are retrieved from Serpent depletion output. The total gap gas composition is then determined as the sum of fill gas and

Table 1
REX Input

Geometry	Fuel radius, cladding thickness, active core height, plenum height, pin pitch, assembly coolant channel radius or apothem, number of assemblies, number of fuel pins per assembly
Coolant properties	Mass flow rate, inlet temperature, boiling point, inlet pressure
Fuel properties	Theoretical density, fuel cycle length
Serpent output	Axially discretized pin fission rates, core nominal power, fuel and fission product isotopic inventories as functions of depletion, number of depletion steps

Table 2
REX Output

Temperatures	Coolant outlet, coolant bulk, cladding inner & outer surfaces, fuel surface, fuel centerline, fuel average
Pressures	Fuel-clad interface, fuel-gas interface, coolant-clad interface
Fuel deformation	Thermal expansion, relocation (cracking), densification, fission product swelling, elasticity, creep
Cladding deformation	Thermal expansion
Mechanics	Cladding maximum allowable and effective stresses

fission product gas particles. Heat transfer from the cladding inner surface to the fuel surface through this gas mixture is modeled as a combination of conduction and radiation [13]. The heat transfer coefficient through the gap is calculated as

$$h_g = \frac{k_{gas}}{\delta_{eff}} + \frac{\sigma_{SB}}{\frac{1}{\varepsilon_f} + \frac{1}{\varepsilon_c} - 1} \frac{T_f^4 - T_{ci}^4}{T_f - T_{ci}} \tag{4}$$

where k_{gas} is the thermal conductivity of the gap gas mixture, δ_{eff} is the effective gap width, σ_{SB} is the Stefan-Boltzmann constant, ε_f and ε_c are the fuel and cladding emissivities, respectively, and T_f is the fuel surface temperature. δ_{eff} is slightly larger than the real gap width due to jump discontinuities in temperature at the fuel-gas and clad-gas interfaces. It is typically modeled as

$$\delta_{eff} = \delta_g + \delta_{jump,f} + \delta_{jump,ci} \tag{5}$$

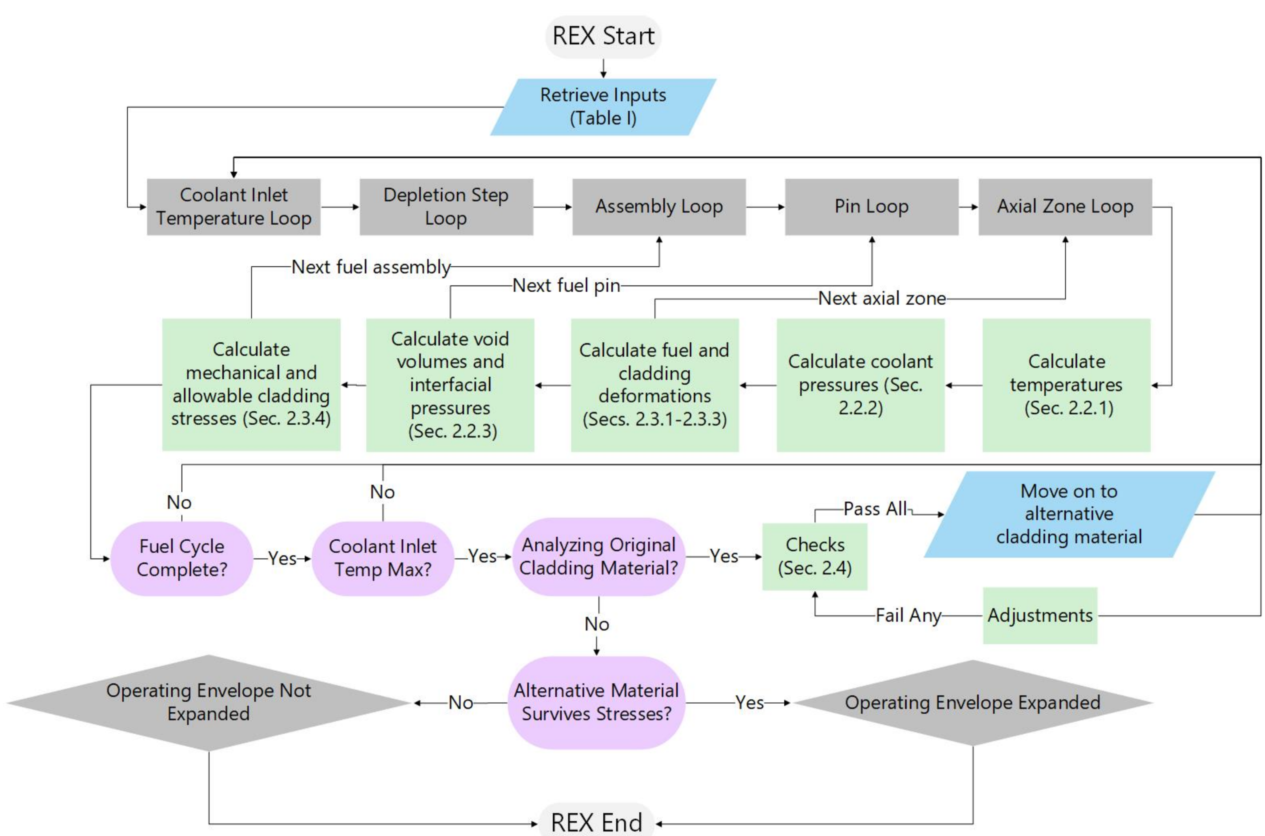

Figure 1: Summary of the REX reactor operating envelope expansion sequence.

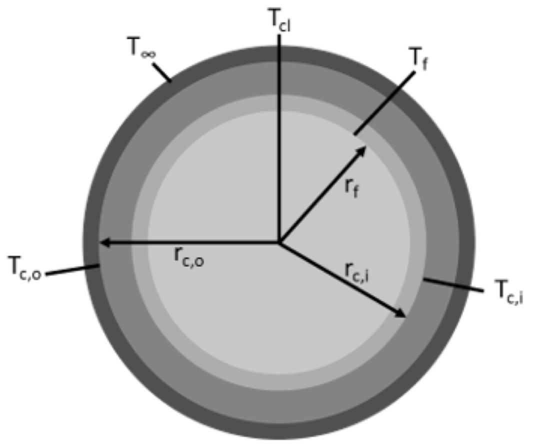

Figure 2: Sample solid cylindrical fuel element with geometry and temperature labels. From the center-outward, each radial segment represents fuel, gap, clad, and coolant, respectively.

where δ_g is the true gap width and $\delta_{jump,f}$ and $\delta_{jump,ci}$ are the gas temperature jump distances at the fuel and inner cladding surfaces, respectively. Gap conductance can also be stated as a function of heat flux, q'', through the gap:

$$h_g = \frac{q''}{T_f - T_{ci}} = \frac{q'''}{T_f - T_{ci}} \frac{r_f}{2} \tag{6}$$

REX numerically solves Eqns. 4 and 6 for the fuel surface temperature, T_f in the presence of a fuel-clad gap.

If a fuel-clad gap is closed or not modeled, REX determines the fuel surface temperature with conduction through an annular surface:

$$T_f = \frac{r_f^2 q'''}{2} \frac{log\left(\frac{r_{co}}{r_f}\right)}{k_{clad}} + T_{co} \tag{7}$$

REX determines T_{cl} by dividing the cross section of the fuel into N discrete radial segments, each with a uniform power density, equal volume, and constant thermal conductivity. The temperature T_{seg} of each radial segment R_{seg} is determined with Eqn. 8:

$$T_{seg+1} = \frac{1}{4}\frac{q'''}{k_{fuel}}\left(R_{seg}^2 - R_{seg+1}^2\right) + T_{seg} \tag{8}$$

where k_{fuel} is the thermal conductivity of the fuel, which REX calculates as a function of porosity, dissolved solid fission products effects, irradiation damage, burnup, and temperature. This iteration has the following boundary conditions:

$$T_{seg} = \begin{cases} T_f, & \text{if } seg = 1 \\ T_{cl}, & \text{if } seg = N \end{cases}$$

and

$$R_{seg} = \begin{cases} r_f, & \text{if } seg = 1 \\ 0, & \text{if } seg = N \end{cases}$$

REX stores the temperatures of every radial fuel segment and uses them to calculate the average fuel temperature, which is used in fission product gas pressure and fuel deformation calculations.

2.2.2. Subchannel Coolant Pressure Losses

Coolant pressures deliver stresses to the cladding at the coolant–clad interface. These pressures experience losses due to acceleration, gravity, and friction as the coolant travels axially through the active region of the core. REX calculates these pressure losses according to [14]. Form losses are also considered and calculated on a case-by-case basis for each reactor design. Presently, REX exclusively considers pressure losses for single-phase coolants traversing axial active regions.

In reactors kept at atmospheric pressure, REX initializes coolant pressure at the inlet of the axial zone as a combination of atmospheric and hydrostatic pressures:

$$P_{cool,in} = P_{atm} + \bar{\rho} g \Delta L \tag{9}$$

where P_{atm} is atmospheric pressure, $\bar{\rho}$ is the average density of the coolant at the inlet and outlet of the axial zone, g is the acceleration due to gravity, and ΔL is the distance from the top of the core to the midplane of the subchannel axial zone.

First, subchannel coolant pressure losses due to axial deceleration are determined with Eqn. 10:

$$-\Delta P_{accl} = \frac{\bar{\rho}}{2}(v_{out}^2 - v_{in}^2) \tag{10}$$

where v_{out} and v_{in} are the inlet and outlet velocities of the coolant in the axial zone.

Next, REX calculates gravitational pressure losses with Eqn. 11:

$$-\Delta P_{grav} = \bar{\rho} g \Delta z \tag{11}$$

where Δz is the height of the axial zone. This quantity will vary as the fuel swells axially.

Third, pressure losses due to friction are calculated with Eqn. 12:

$$-\Delta P_{fric} = f \frac{\Delta z}{D_e} \frac{\bar{\rho}\bar{v}^2}{2} \tag{12}$$

where $\bar{v}$ is the average coolant velocity in the axial zone, D_e is the subchannel equivalent diameter, and f is the flow friction factor. REX calculates f in each axial zone as a function of the average Reynolds number $\overline{Re}$ with the Blasius and McAdams correlations [15].

$$f = \begin{cases} \frac{64}{\overline{Re}}, & \overline{Re} < 2200 \\ 0.316\overline{Re}^{-0.25}, & 2200 < \overline{Re} < 30,000 \\ 0.184\overline{Re}^{-0.20}, & \overline{Re} > 30,000 \end{cases} \tag{13}$$

The three pressure loss terms calculated in Eqns. 10–12 are combined for a total pressure loss:

$$\Delta P_{total} = \Delta P_{accl} + \Delta P_{grav} + \Delta P_{fric} \tag{14}$$

REX calculates these pressure losses for every axial zone in every subchannel in the core. The resulting axial pressure profile is used in conjuntion with fission product gas pressure (Sec. 2.2.3) and fuel-clad interfacial pressure (Sec. 2.3.3) to determine the effective stress experienced by the cladding (Sec. 2.3.4). The assumption of no crossflow will affect the accuracy of these calculations to an extent that will be determined in future validation studies.

2.2.3. Fission Product Gas Release and Pressure

As the molecular composition of the fuel changes at high temperature, accumulated fission product gases are released into the fuel-clad gap (if one exists) and the gas plena and pressurize the cladding inner surface. The number of fission product gas atoms produced in every fuel pin as a function of depletion is retrieved from the depletion output produced by Serpent. In the case of UO_2 fuel, REX estimates the release fraction of these particles from the entire fuel pin with the following empirical relation [16]:

$$f_{release} = \begin{cases} 0.05, & T < 1400\ °C \\ 0.10, & 1400\ °C < T < 1500\ °C \\ 0.20, & 1500\ °C < T < 1600\ °C \\ 0.40, & 1600\ °C < T < 1700\ °C \\ 0.60, & 1700\ °C < T < 1800\ °C \\ 0.80, & 1800\ °C < T < 2000\ °C \\ 0.98, & T > 2000\ °C \end{cases} \tag{15}$$

where T is the average fuel pin temperature.

The pressure due to the mixture of fission product gases and the fuel-clad gap fill gas affects the fuel elastic deformations observed during closed fuel-clad gap scenarios [17]. REX determines this fuel-gas interfacial pressure for every event of fuel-clad gap closure in the fuel pin. For this calculation, a continuous cluster of axial zones in which the fuel-clad gap has been closed is treated as a single *closure* and each cluster of non-closures is deemed a *void*. REX assumes gas particles are distributed into each void, proportional to the void volume, and calculates the gas pressure in each void with the ideal gas law:

$$P_{gas} = \frac{N_{gas} k_B T}{V_{void}} \tag{16}$$

where $N_{gas} = N_{FP} + N_{fill}$ is the number of fission product and fill gas particles in the void, T is the average temperature of the pin, k_B is the Boltzmann constant, and V_{void} is the volume of the void. The fuel slice at the border of each void-closure interface is then assumed to experience the gas pressure in its respective void. In the event of complete fuel-clad gap closure, as is the case in later depletion steps, all of the gas is assumed to reach the upper and lower gas plena and pressurize the axial top and bottom fuel surfaces. This void-closure treatment is illustrated in Fig. 3.

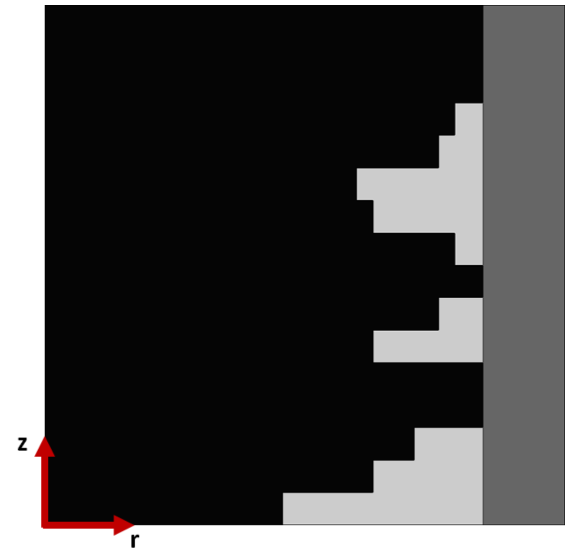

Figure 3: Visualization of void-closure treatment of radial fuel swelling and fuel-clad gap closure in discrete axial zones. Black, light gray, and dark gray regions represent fuel, gap, and clad, respectively. z and r denote the axial and radial coordinates, respectively. Not to scale.

2.3. Thermo-Mechanics

2.3.1. Fuel Deformation

REX calculates radial and axial fuel swelling due to the following mechanisms: thermal expansion, cracking due to thermal stresses (termed *relocation*), densification, and swelling due to the appearance of solid and gaseous fission products. The rates of these swelling mechanisms depend on fuel composition. As of the date of this paper, only UO_2 fuel deformation has been incorporated into REX. Fuel deformations due to thermal expansion and relocation are calculated as linear strains and are applied to the fuel radius and height at each axial zone. Densification and swelling due to fission products, however, are volumetric strains and are calculated for entire fuel pins.

2.3.2. Cladding Thermal Expansion

REX also considers radial and linear swelling of the cladding material due to thermal expansion with the canonical formula:

$$\left(\frac{\Delta L}{L}\right)_{clad} = \alpha_{clad} \left(\Delta T\right)_{clad} \tag{17}$$

where α_{clad} is the coefficient of thermal expansion of the cladding, $(\Delta T)_{clad}$ is the change in cladding temperature at each depletion step, and $\left(\frac{\Delta L}{L}\right)_{clad}$ is the fractional change in length of the cladding material.

2.3.3. Fuel-Clad Mechanical Interactions and the Soft Pellet Model

REX considers the fuel and cladding to be in “hard contact” after two conditions are met:

1. Fuel fully traverses the fuel-clad gap.

2. 50% of the fuel relocation strain is recovered by the combination of fuel and cladding radial strains.

At hard contact, REX quantifies pellet-clad mechanical interactions (PCMI) with the Soft Pellet Model, an iterative sequence that yields fuel-clad interfacial pressure for cladding stress calculations [17]. The model starts with two continuity conditions. First, radial continuity dictates that fuel and cladding radial displacements must be equal. Second, axial continuity requires that additional axial strain in the fuel is transferred entirely to the cladding. These conditions are described by Eqns. 18 and 19, respectively:

$$\text{Radial continuity:} \qquad u_{fo} = u_{ci} \tag{18}$$

$$\text{Axial continuity:} \quad \varepsilon_z^{clad} - \varepsilon_{z,0}^{clad} = \varepsilon_z^{fuel} - \varepsilon_{z,0}^{fuel} \tag{19}$$

where u_{fo} is the outer radial displacement of the fuel, u_{ci} is the inner radial displacement of the cladding, ε_z denotes axial strain, and $\varepsilon_{z,0}$ denotes axial strain at contact. REX uses these conditions to determine the tangential (hoop) stress on the cladding, assuming the cladding is a thin-walled cylindrical shell:

$$\sigma_\theta = \frac{E\left(2u_{ci} - \varepsilon_z \nu (t - 2\tilde{r})\right)}{2\tilde{r} + \nu (t + \nu t + 2\tilde{r}\nu)} \tag{20}$$

where E is the elastic modulus of the cladding material, ν is the Poisson ratio of the cladding material, t is the thickness of the cladding, and $\tilde{r} = \frac{r_{co}+r_{ci}}{2}$. REX uses the cladding hoop stress to obtain an initial guess at the fuel-clad interfacial pressure:

$$P_{int} = \frac{t\sigma_\theta + r_{co}P_{cool}}{r_{ci}} \tag{21}$$

where P_{cool} is the coolant pressure in the axial zone, described in Sec. 2.2.2. Fuel-clad interfacial pressures induce plastic deformations in the fuel (hence the name, "Soft Pellet Model"). REX calculates the radial and axial components of this strain with Eqns. 22 and 23:

$$\varepsilon_{rf} = \frac{\nu_f P_{gas} - P_{int}}{E_f} \tag{22}$$

$$\varepsilon_{zf} = \frac{\nu_f P_{int} - P_{gas}}{E_f} \tag{23}$$

where ε_{rf} and ε_{zf} are the radial and axial elastic fuel strains due to PCMI, P_{gas} is the fuel-gas interfacial pressure described in Sec. 2.2.3, P_{int} is the fuel-clad interfacial pressure, E_f is the fuel elastic modulus, and ν_f is the fuel Poisson ratio. With these parameters, REX completes its first iteration of the Soft Pellet Model by calculating the additional fuel radial displacement due to elastic deformations:

$$u_{fo} = r_f \varepsilon_{rf} \tag{24}$$

REX then loops through Eqns. 18–24 until it converges on a solution for the fuel-clad interfacial pressure, P_{int}, for the current axial zone.

2.3.4. *Cladding Mechanical Response*

REX uses the coolant-clad, gas-clad, and fuel-clad interfacial pressures determined in Sec. 2.2.2, Sec. 2.2.3, and Sec. 2.3.3, respectively, to determine the radial, tangential, and axial stresses experienced by the cladding [18]:

$$\sigma_{rc} = \frac{P_{int}r_f^2 - P_{cool}r_{co}^2 + \frac{r_f^2 r_{co}^2 (P_{cool} - P_{int})}{r^2}}{r_{co}^2 - r_f^2} \tag{25}$$

$$\sigma_{\theta c} = \frac{P_{int}r_f^2 - P_{cool}r_{co}^2 - \frac{r_f^2 r_{co}^2 (P_{cool} - P_{int})}{r^2}}{r_{co}^2 - r_f^2} \tag{26}$$

$$\sigma_{zc} = \frac{P_{int}r_f^2 - P_{cool}r_{co}^2}{r_{co}^2 - r_f^2} \tag{27}$$

where σ_{rc}, $\sigma_{\theta c}$, and σ_{zc} are the radial, tangential, and axial stresses experienced by the cladding at the current axial zone. r is the radial point where the stress is evaluated, which is chosen to be r_f. REX combines these three stress components to calculate the effective stress delivered to the cladding with the Von Mises equation:

$$\sigma_e = \sqrt{(\frac{\left(\sigma_{zc} - \sigma_{\theta c}\right)^2 + \left(\sigma_{\theta c} - \sigma_{rc}\right)^2 + \left(\sigma_{rc} - \sigma_{zc}\right)^2}{2}} \tag{28}$$

REX compares this effective stress to the maximum allowable stress, which is a function of the cladding material. To identify the base operating envelope of the reactor with the original cladding material, REX will manipulate fuel pin geometries to ensure that the effective stress exceeds the maximum allowable stress at the final depletion step and maximum allowable coolant inlet temperature. This manipulation is described in Sec. 2.4.

2.4. Adjustments to Fuel Pin Geometry

At the end of its calculation for the reactor outfitted with the original cladding material, REX locates the fuel pin that experiences the most swelling and determines the following:

- Predicted fuel swelling past the cladding outer wall:

$$\Delta r_{cx} = r_f - r_{co}$$

- Excess fuel swelling beyond the gap:

$$\Delta r_{gx} = r_f - r_{ci}$$

- Excess cladding stress:

$$\Delta \sigma_x = \sigma_e - \sigma_{lim}$$

where σ_{lim} is the stress limit of the cladding. REX uses these three parameters to perform a series of checks and adjustments to the fuel pin geometries:

Table 3
FHR Core Parameters

Core thermal power	125 MW
Number of assemblies	91
Fuel pins per assembly	60
Fuel type	UO_2, 18.8 wt% ^{235}U
Original cladding material	SiC
Moderator material	Graphite
Reflector material	Graphite
Coolant	Li_2Be_4F (FLiBe)
Coolant boiling point	1430 °C
Coolant inlet temperature	700 °C
Fuel cycle length	395 EFPD
Cold fuel radius	0.477 cm
Cladding thickness	0.057 cm
Active height	400 cm
Fuel pin pitch	1.944 cm
Assembly pitch	20 cm

1. If $\Delta r_{cx} > 0$, the fuel-clad gap is extended to accommodate the excess fuel swelling.
2. If $\Delta r_{cx} < 0$, $\Delta r_{gx} > 0$, and $\Delta \sigma_x > 0$, the cladding thickness is extended.
3. If $\Delta r_{cx} < 0$, $\Delta r_{gx} > 0$, and $\Delta \sigma_x < 0$, the cladding thickness is decreased.
4. If $\Delta r_{gx} < 0$, the fuel-clad gap is decreased by 50% to force fuel-clad contact in the next iteration.
5. If several iterations result in the fuel-clad gap being decreased by 50%, REX will adjust the cladding thickness so that clad occupies nearly the entire fuel pin pitch. This adjustment potentially forces $\Delta \sigma_x < 0$ for remaining iterations.

After an adjustment, REX repeats the entire calculation sequence to retrieve a new operating envelope with the updated fuel pin geometries. This iteration is repeated until REX determines the fuel pin geometries that give rise to a minimum positive value of $\Delta \sigma_x$ at the end of the fuel cycle with maximum coolant inlet temperature. REX then uses these geometries to perform all thermal-hydraulic and thermo-mechanical calculations for the reactor outfitted with the alternative cladding materials and compares the effective and maximum allowable stresses for each case.

3. Example Analysis of a Fluoride Salt-Cooled High Temperature Reactor

3.1. FHR Summary

REX was used to analyze and potentially expand the thermo-mechanical operating envelope of a small, pin-type fluoride salt-cooled high-temperature reactor (FHR) with the PCMI methodology. The FHR design is detailed in [19] and briefly summarized here. Essential core details are provided in Table 3 and an illustration of the FHR core and fuel assembly is shown in Fig. 4. The FHR in this example study had received preliminary coupled neutronic-thermal hydraulic analysis by [19]. The Li_2Be_4F (FLiBe)-cooled 125-MWt core contains 91 hexagonal fuel assemblies, each containing 60 solid cylindrical uranium dioxide (UO_2) fuel pins surrounded by silicon carbide (SiC) cladding. Each assembly is centered by a SiC tie rod, embedded in a graphite moderator matrix, and arranged in a hexagonal lattice surrounded by a cylindrical graphite reflector. This FHR had only previously received neutronic and preliminary thermal-hydraulic analysis; therefore, no fuel-clad gap was specified in design literature, rendering this FHR a suitable model for REX.

Table 4
FHR Run Parameters Used in Serpent

Model type	Axially-infinite core
Number of axial segments	16
Neutrons per generation	350,000
Active generations	200
Skipped generations	20
Depletion steps (total days)	0.1, 1, 5 to 395 in 10-day increments
Tallied fissile elements	Th, Pa, Minor Actinides
Tallied fission product gases	Kr, Xe, I, Br, Cs, Te

3.2. FHR Simulation

The neutronics of the small, 125-MWt FHR were simulated with the Serpent 2 Monte Carlo neutron transport code. Serpent was used to analyze an axially infinite core and score fission rates in 16 equally spaced axial zones along a height of 400 cm. Each of the 91 fuel assemblies are modeled with their own identical yet distinguishable fuel material for the collection of assembly-specific depletion statistics. The depletion steps and neutron population statistics for this simulation are presented in Table 4. Several depletion steps were simulated for precise evolution of the cladding stress profiles with time. All isotopes of thorium, palladium, and the minor actinides were tallied in each assembly for an accurate description of fuel evolution, which is used to compute burnup in atom percent, a necessary parameter for several correlations described in Sec. 2. Additionally, the inventory of fission products that appear as gases at FHR temperatures was collected for use in Eqn. 16.

3.3. FHR Results

The adjustments made to the geometries of the limiting FHR fuel pin, as described in Sec. 2.4, are shown in Fig. 5. REX automatically determines optimal initial values of fuel-clad gap width and cladding thickness for the limiting fuel pin to force a maximum effective stress that narrowly exceeds the SiC fracture stress. These final geometries and corresponding stresses are provided in Table 5.

The effective and maximum allowable SiC stresses with these geometries are plotted in Fig. 6. Because SiC is a brittle material, its maximum allowable stress is its fracture strength [20]. The effective stress of the original cladding material, SiC, exceeds the maximum allowable stress at the final depletion step and maximum coolant inlet temperature,

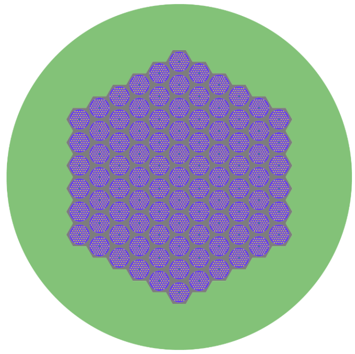

(a) FHR core

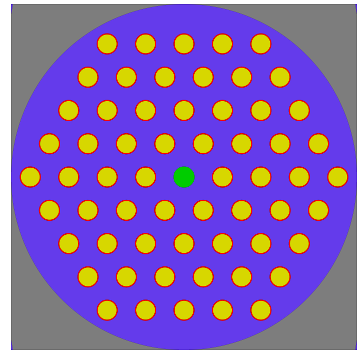

(b) FHR fuel assembly

Figure 4: FHR geometry plots produced with Serpent. The green disk in 4a is the reflector. Purple, yellow, red, and gray in 4b are coolant, fuel, cladding, and moderator, respectively. The central green pin is a SiC tie rod.

Table 5
FHR Limiting Pin Initial and Adjusted Parameters

	Initial Design	REX Output
Gap width (μm)	0	85
Cladding thickness (μm)	570	8091.49
Effective stress (MPa)	7650.37	809.07
Stress limit (MPa)	787.3359	809.01

indicating that REX has identified the base operating envelope for this FHR with the limiting fuel pin geometries listed in Table 5.

Finally, consider an alternative cladding material: Inconel 718, a nickel alloy. The mechanical response of this material as fuel cladding in the FHR is shown in Fig. 7. Because Inconel 718 is a ductile material, its maximum allowable stress is its yield strength [21]. The Inconel 718 profile exhibits both a large drop in yield strength and an intersection between effective stress and yield strength. These observations suggest that Inconel is not a suitable composite to expand the envelope of the FHR; the material experiences a prohibitive Von Mises stress profile before the operational limit of the original SiC cladding is met.

4. Conclusions and Future Work

REX, an analytical reactor design tool, was developed to automatically identify and expand the operating envelopes of advanced solid-fuel nuclear reactor cores based on their fuel-clad, fuel-gas, and coolant-clad thermo-mechanics. With reactor geometry, coolant inlet temperature, and axially discretized detector and depletion results from Serpent as its inputs, REX performs full-core, pin-specific thermal-hydraulic and thermo-mechanical calculations to determine cladding mechanical stresses as functions of fuel depletion and coolant inlet temperature. It pushes the reactor operating envelope by increasing coolant inlet temperature until the coolant boiling point or cladding temperature limit is reached. It then modifies fuel pin geometries to induce mechanical failure of the original cladding material at the full extent of the fuel cycle and maximum permissible coolant inlet temperature. REX then replaces the original cladding with candidate alternative cladding materials specified by the user and evaluates their capability to expand the reactor operating envelope by testing their performance with the limiting fuel pin geometry.

REX is currently capable of analyzing reactor concepts outfitted with the fuels, coolants, and cladding materials listed in Table 6. Also listed are planned additions. REX is consistently being updated to improve both the accuracy and breadth of its calculation sequence. Future work will consist of the following items:

- The materials & coolants library will continue to be expanded with additional fuels, cladding materials, and coolants.
- The calculation of cladding wall thinning will be incorporated as a function of cladding identity, coolant identity, coolant temperature, and cladding-coolant exposure time.
- The validity and accuracy of the REX output must be assessed with validation and verification benchmarks. Specifically, the effects of changing the cladding thickness, cladding material, and fuel-clad gap width should be verified with the fuel rod behavioral analysis codes referenced in Sec. 1.
- To increase accessibility, REX will be rebuilt in Python and expanded to work with neutronic results from MCNP-based codes.

Reactors concepts subject to future analysis are the lead-cooled flexible conversion ratio reactor [3] and the AFR-100 sodium-cooled fast reactor [22].

5. Acknowledgements

The information, data, or work presented herein was funded in part by the Advanced Research Projects Agency – Energy (ARPA-E), U.S. Department of Energy, under Award Number DE-AR0001066. The views and opinions of authors

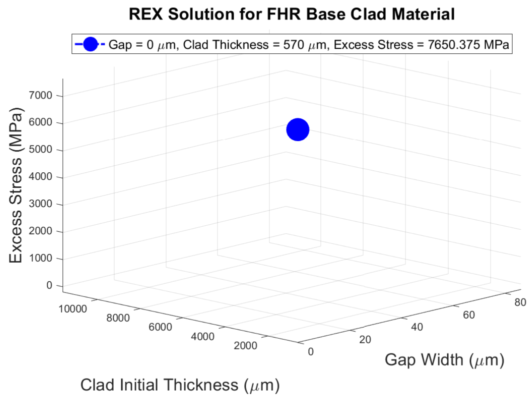

(a) Initial specifications

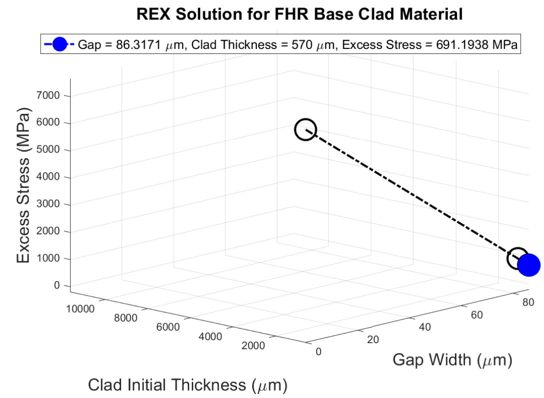

(b) Fuel-clad gap extension

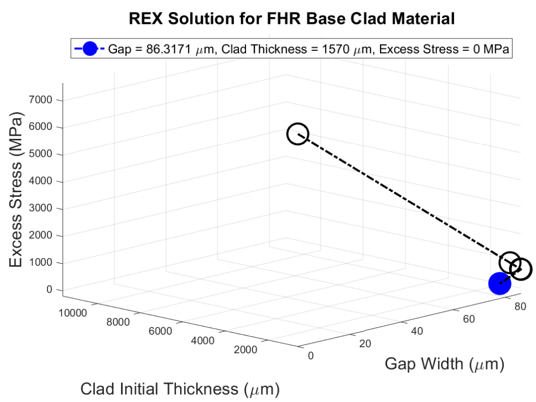

(c) Clad thickness extension (no fuel-clad contact)

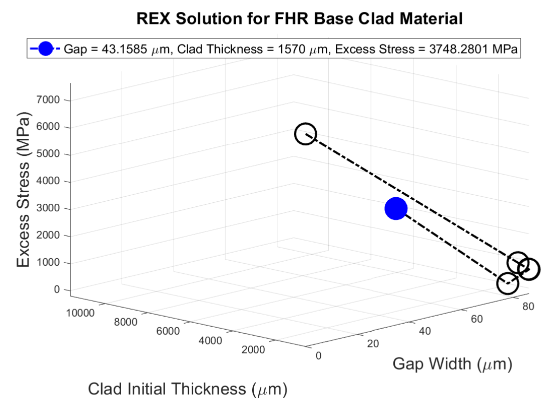

(d) 50% fuel-clad gap reduction

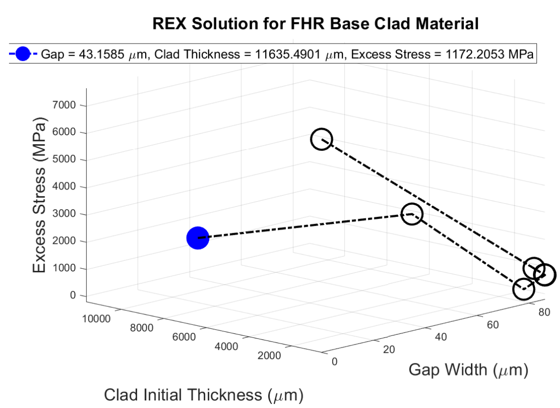

(e) Clad thickness maximization

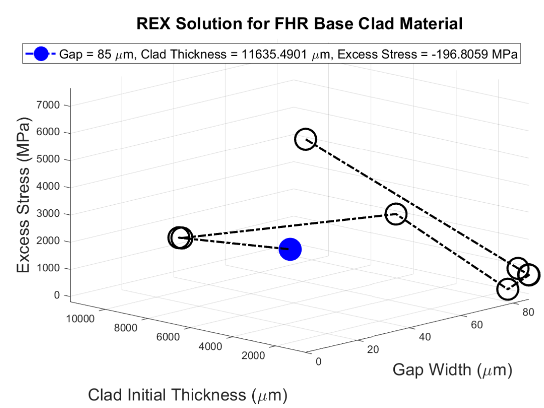

(f) Fuel-clad gap extension

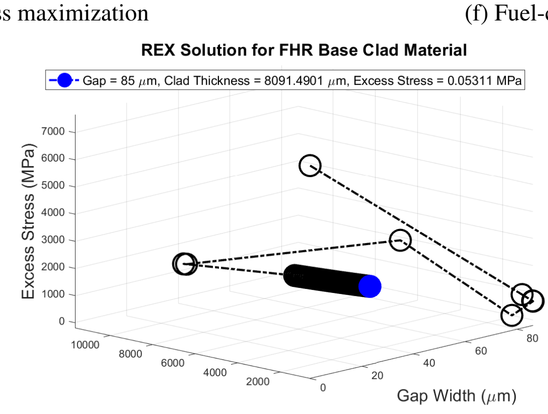

(g) Clad thickness reduction

Figure 5: Convergence on ideal geometries to narrowly force cladding fracture in the limiting FHR fuel pin. REX performs these modifications automatically according to checks described in Sec. 2.4.

Table 6
REX Materials & Coolants Library

	Current	In Progress	Planned
Fuels	UO_2, MOX		UN, UC, NatU, Th
Clads	SiC, Ni-201, Inconel 718, INCOLOY 800H, HAYNES alloy 230, T91 steel, 316L stainless steel	HT9 steel, Zircaloy-4	ODS steel, Graphite
Coolants	Lead, LBE, Sodium, FLiBe, FLiNaK, He	H_2O	D_2O, CO_2

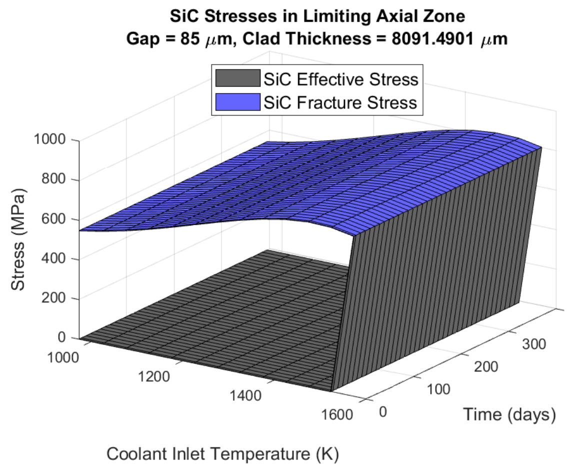

Figure 6: SiC effective stress (gray) and fracture strength (blue) with limiting fuel pin geometry. The spike and subsequent drop in stress at the beginning of the fuel cycle are due to fuel densification.

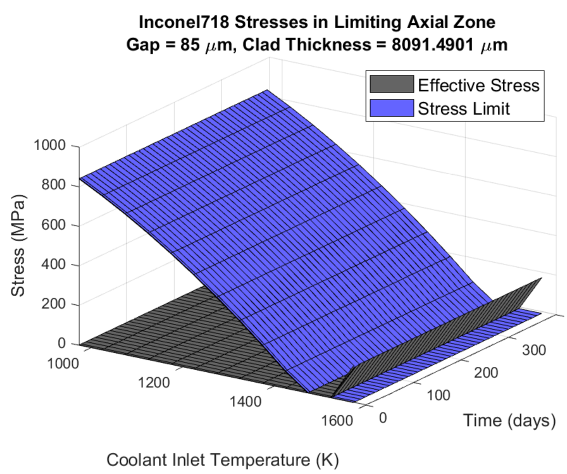

Figure 7: Attempted FHR operating envelope expansion with Inconel 718. Effective stress (gray) exceeds yield strength (blue) after yield strength drops to zero due to temperature effects.

expressed herein do not necessarily state or reflect those of the United States Government or any agency thereof.

The authors would like to thank Professor Michael Short, Class of '42 Associate Professor of Nuclear Science and Engineering at the Massachusetts Institute of Technology, for his support, discussion, and feedback.

6. Disclaimer

The information, data, or work presented herein was funded in part by an agency of the United States Government. Neither the United States Government nor any agency thereof, nor any of their employees, makes any warranty, express or implied, or assumes any legal liability or responsibility for the accuracy, completeness, or usefulness of any information, apparatus, product, or process disclosed, or represents that its use would not infringe privately owned rights. Reference herein to any specific commercial product, process, or service by trade name, trademark, manufacturer, or otherwise does not necessarily constitute or imply its endorsement, recommendation, or favoring by the United States Government or any agency thereof. The views and opinions of authors expressed herein do not necessarily state or reflect those of the United States Government or any agency thereof.

List of Symbols

$T_\infty \equiv$ Coolant bulk temperature
$T_{co} \equiv$ Cladding outer surface temperature
$T_{ci} \equiv$ Cladding inner surface temperature
$T_f \equiv$ Fuel surface temperature
$T_{cl} \equiv$ Fuel centerline temperature
$T_{cool,in} \equiv$ Coolant inlet temperature
$q''' \equiv$ Power density
$V \equiv$ Axial slice volume
$c_p \equiv$ Coolant isobaric heat capacity
$r_f \equiv$ Fuel radius
$r_{co} \equiv$ Cladding outer radius
$h \equiv$ Convective heat transfer coefficient
$r_{ci} \equiv$ Cladding inner radius
$k_{clad} \equiv$ Cladding thermal conductivity
$h_g \equiv$ Fuel-clad gap heat transfer coefficient
$k_{gas} \equiv$ Fuel-clad gap gas thermal conductivity
$\dot{m}_{sub} \equiv$ Axial slice coolant mass flow rate
$\delta_{eff} \equiv$ Effective gap width
$\sigma_{SB} \equiv$ Stefan-Boltzmann constant
$\epsilon_f, \epsilon_c \equiv$ Fuel and cladding emissivities, respectively
$\delta_g \equiv$ True gap width
$\delta_{jump,f} \equiv$ Fuel surface gas temperature jump distance
$\delta_{jump,ci} \equiv$ Inner clad surface gas temperature jump distance
$T_{seg} \equiv$ Fuel radial segment temperature
$k_{fuel} \equiv$ Fuel thermal conductivity
$R_{seg} \equiv$ Fuel radial segment width
$P_{cool,in} \equiv$ Coolant inlet pressure
$P_{atm} \equiv$ Atmospheric pressure

$\bar{\rho} \equiv$ Axial slice average coolant density
$g \equiv$ Acceleration due to gravity
$\Delta L \equiv$ Distance from axial slice mid-plane to core outlet
$\Delta P_{accl} \equiv$ Acceleration pressure losses
$v_{out} \equiv$ Axial slice coolant outlet velocity
$v_{in} \equiv$ Axial slice coolant inlet velocity
$\Delta P_{grav} \equiv$ Gravitational pressure losses
$\Delta z \equiv$ Axial slice height
$\Delta P_{fric} \equiv$ Frictional pressure losses
$\bar{v} \equiv$ Axial slice average coolant velocity
$D_e \equiv$ Subchannel equivalent diameter
$\underline{f} \equiv$ Coolant flow friction factor
$Re \equiv$ Axial slice average coolant Reynolds number
$\Delta P_{total} \equiv$ Total pressure loss
$f_{release} \equiv$ Fission product gas release fraction
$P_{gas} \equiv$ Void gas pressure
$N_{gas} \equiv$ Void total fission product and fill gas particles
$k_B \equiv$ Boltzmann constant
$\left(\frac{\Delta L}{L}\right)_{clad} \equiv$ Fractional change in cladding length
$\alpha_{clad} \equiv$ Cladding coefficient of thermal expansion
$u_{fo} \equiv$ Fuel outer radial displacement
$u_{ci} \equiv$ Cladding inner radial displacement
$\varepsilon_z \equiv$ Axial strain
$\varepsilon_{z,0} \equiv$ Axial strain at fuel-clad contact
$\sigma_\theta \equiv$ Hoop stress
$E \equiv$ Elastic modulus
$\nu \equiv$ Poisson's ratio
$t \equiv$ Cladding thickness
$P_{int} \equiv$ Fuel-clad interfacial pressure
$P_{cool} \equiv$ Axial slice coolant pressure
$\varepsilon_f \equiv$ Elastic fuel strain
$P_{gas} \equiv$ Fuel-gas interfacial pressure
$\sigma_r \equiv$ Radial stress
$\sigma_z \equiv$ Axial stress
$\sigma_e \equiv$ Von Mises stress
$\Delta r_{cx} \equiv$ Excess fuel swelling beyond cladding outer wall
$\Delta r_{gx} \equiv$ Excess fuel swelling beyond cladding inner wall
$\Delta\sigma_x \equiv$ Excess cladding stress

References

[1] Aashique A. Rezwan, Michael R. Tonks, and Michael P. Short. Evaluations of the performance of multi-metallic layered composite cladding for the light water reactor accident tolerant fuel. *Journal of Nuclear Materials*, 535:152136, 2020.

[2] Michael Philip Short and Ronald George Ballinger. A functionally graded composite for service in high-temperature lead- and lead-bismuth–cooled nuclear reactors—i: Design. *Nuclear Technology*, 177(3):366–381, 2012.

[3] Anna Nikiforova, Pavel Hejzlar, and Neil E. Todreas. Lead-cooled flexible conversion ratio fast reactor. *Nuclear Engineering and Design*, 239(12):2596–2611, 2009. Flexible Conversion Fast Reactors Special Section with Regular Papers.

[4] Govindarajan Muralidharan, Dane F Wilson, Michael L Santella, and David Eugene Holcomb. Cladding alloys for fluoride salt compatibility final report. (ORNL/TM-2011/95), 5 2011.

[5] EPRI. Fuel analysis and licensing code: FALCON MOD01: Volume 1: Theoretical and numerical bases. 2004.

[6] C.M. Allison, G.A. Berna, R. Chambers, E. W. Coryell, K.L. Davis, D.L. Hagrman, D.T. Hagrman, N.L. Hampton, J.K. Hohorst, R.E. Mason, M.L. McComas, K.A. McNeil, R.L. Miller, C.S. Olsen, G.A. Reymann, and L.J. Siefken. SCDAP/RELAP5/MOD3.1 code manual: MATPRO–a library of materials properties for light-water reactor accident analysis. 6 1995.

[7] Yong-Jun Deng, Jun Wei, Yang Wang, and Bin Zhang. Validation of the fuel rod performance analysis code fripac. *Nuclear Engineering and Technology*, 51(6):1596–1609, 2019.

[8] Kenneth Geelhood, Walter Luscher, Patrick Raynaud, and Ian Porter. FRAPCON-4.0: A computer code for the calculation of steady-state, thermal-mechanical behavior of oxide fuel rods for high burnup. (PNNL-19418, Vol.1 Rev.2):1.1–1.2, 09 2015.

[9] J. D. Hales, R. L. Williamson, S. R. Novascone, G. Pastore, B. W. Spencer, D. S. Stafford, K. A. Gamble, D. M. Perez, and W. Liu. BISON theory manual the equations behind nuclear fuel analysis. (INL/EXT-13-29930):4, 9 2016.

[10] Isabelle Guénot-Delahaie, J. Sercombe, Thomas Helfer, Patrick Goldbronn, Eric Fédérici, Thomas Jolu, Aurore Parrot, Delafoy Christine, and Christian Bernaudat. Simulation of ria transients on uo2-m5® fuel rods with alcyone v1.4 fuel performance code. 09 2017.

[11] Jaakko Leppänen, Maria Pusa, Tuomas Viitanen, Ville Valtavirta, and Toni Kaltiaisenaho. The serpent monte carlo code: Status, development and applications in 2013. *Annals of Nuclear Energy*, 82:142–150, 2015. Joint International Conference on Supercomputing in Nuclear Applications and Monte Carlo 2013, SNA + MC 2013. Pluri- and Trans-disciplinarity, Towards New Modeling and Numerical Simulation Paradigms.

[12] N. Kaffezakis and D. Kotlyar. Fuel cycle analysis of novel assembly design for thorium-uranium-ceramic–fueled thermal, high-conversion reactor. *Nuclear Technology*, 206(1):48–72, 2020.

[13] Neil E. Todreas and Mujid S. Kazimi. *Nuclear Systems I: Thermal Hydraulic Fundamentals*, pages 332–334. Taylor & Francis, 1989.

[14] Neil E. Todreas and Mujid S. Kazimi. *Nuclear Systems I: Thermal Hydraulic Fundamentals*, page 581. Taylor & Francis, 1989.

[15] Neil E. Todreas and Mujid S. Kazimi. *Nuclear Systems I: Thermal Hydraulic Fundamentals*, page 379. Taylor & Francis, 1989.

[16] Neil E. Todreas and Mujid S. Kazimi. *Nuclear Systems I: Thermal Hydraulic Fundamentals*, pages 305–306. Taylor & Francis, 1989.

[17] Bo-Shiuan Li. Pellet cladding mechanical interactions of ceramic claddings fuels under light water reactor conditions. Master's thesis, University of South Carolina, 2013.

[18] Kenneth Geelhood, Walter Luscher, Patrick Raynaud, and Ian Porter. FRAPCON-4.0: A computer code for the calculation of steady-state, thermal-mechanical behavior of oxide fuel rods for high burnup. (PNNL-19418):2.32–2.33, 09 2015.

[19] Hassan Mohamed, Dan Kotlyar, Geoffrey Parks, and Yaniv Shaposhnik. Coupled neutronic-thermal-hydraulic analysis of a small FHR core with pin-type fuel assemblies. PHYSOR 2014:1–5, 2014.

[20] Nasr M. Ghoniem. High-temperature mechanical and material design for SiC composites. *Journal of Nuclear Materials*, 191-194:515–519, 1992. Fusion Reactor Materials Part A.

[21] Special Metals. Inconel alloy 718. pages 1–2,10. https://www.specialmetals.com/documents/Inconelalloy718.pdf Accessed 1 April 2021.

[22] Christopher Grandy, James J. Sienicki, Anton Moisseytsev, Lubomir Krajtl, Mitchell T. Farmer, Taek K. Kim, and B. Middleton. Advanced fast reactor - 100 (AFR-100) report for the technical review panel. ANL-ARC-288, 6 2014.